

THU-93/12

Effects of negative energy components in the constituent quark model

Peter C. Tiemeijer and J.A. Tjon

Institute for Theoretical Physics, University of Utrecht, Box 80.006, 3508 TA Utrecht, The Netherlands.

Abstract

Relativistic covariance requires that in the constituent quark model for mesons the positive energy states as well as the negative energy states are included. Using relativistic quasi-potential equations the contribution of the negative energy states is studied for the light and charmonium mesons. It is found that these states change the meson mass spectrum significantly but leave its global structure untouched.

PACS numbers: 12.35.H, 12.40.Q, 11.10.Q

Typeset using REVTEX

I. INTRODUCTION

The application of the constituent quark model to mesons and baryons has been very successful, in spite of various nonrelativistic approximations. How much is neglected in these approximations? Generalization of the ordinary Schrödinger equation to a relativistic covariant form results in the well-known Bethe-Salpeter equation (BSE), which differs from the nonrelativistic equation in two respects. Firstly, the dependence of the bound state wave function on the relative three-momentum \mathbf{p} becomes a dependence on the four-momentum (p_0, \mathbf{p}) . Secondly, covariance requires that for fermions the full Dirac structure is taken into account, so for quarks not only the positive energy states are to be considered, but also their negative energy states must be included. In this paper we investigate the effect on the meson mass spectrum of the inclusion of these negative energy states in the relativistic constituent quark model.

Quasi-potential (QP) approximations to the BSE exist which eliminate the p_0 -dependence of the quark-propagators, and moreover circumvent the problem of introducing a confining potential in the full Minkowski space. The covariant Dirac structure is kept in these. In previous work [1,2], to which we shall refer as I and II, we used two QP models to calculate the full meson mass spectrum. One of the biggest differences found with the Schrödinger approach was the much stronger confinement needed and the sensitivity of the mass spectrum to small vector contributions to the confining potential. To get some more insight about the various aspects we have performed calculations in the same framework but with leaving out various negative energy states. This enables us to trace back and understand the origin of the phenomena found in I and II and to establish the importance of the negative energy states. For simplicity the calculations are restricted to the equal mass case.

In the next section the model is briefly summarized and some of the QP equations properties which give upper bounds on the parameters of the potential are discussed. Section III deals with the truncation of the relativistic QP equations in the coordinate representation with regards to the negative energy spinor states. It also presents the comparison of the calculations with corresponding nonrelativistic predictions. In particular the $u\bar{u}$ and $c\bar{c}$ spectra are considered in various approximations to various QP models. Differences in the spectra are discussed. Finally, the paper closes with some concluding remarks.

II. REVIEW OF MODEL

We briefly describe the relativistic constituent quark model as was studied in I and II. The model consists of two point-like fermions bound together by a phenomenological potential V to form a meson. The meson wave function ψ satisfies

$$S^{-1}(\mathbf{p})\psi(\mathbf{p}) = - \int \frac{d\mathbf{q}}{(2\pi)^3} V(\mathbf{p} - \mathbf{q})\psi(\mathbf{q}). \quad (2.1)$$

The dependence of the propagator S on the relative four-momentum (p_0, \mathbf{p}) has been simplified to a dependence on the three-momentum. In I we studied two QP approximations which eliminate the dependence of the equation on p_0 , the Blankenbecler-Sugar-Logunov-Tavkhelidze (BSLT) approximation [3,4], and an equal-time (ET) approximation [5,6]. They give for quarks of equal mass in the center of mass system

$$S_{BSLT}^{-1}(\mathbf{p}) = 4\omega \left[\frac{\omega - E}{\omega + E} \Lambda^{++} - \Lambda^{+-} - \Lambda^{-+} + \frac{\omega + E}{\omega - E} \Lambda^{--} \right], \quad (2.2)$$

and

$$S_{ET}^{-1}(\mathbf{p}) = 2(\omega - E)\Lambda^{++} - 2\omega(\Lambda^{+-} + \Lambda^{-+}) + 2(\omega + E)\Lambda^{--}, \quad (2.3)$$

where $\omega = \sqrt{\mathbf{p}^2 + m^2}$, and $E = M/2$, M being the total meson mass. The $\Lambda^{\rho_1\rho_2}$ project upon positive and negative energy states, $\Lambda^{\rho_1\rho_2} = \Lambda_1^{\rho_1}(\mathbf{p})\Lambda_2^{\rho_2}(-\mathbf{p})$ with

$$\Lambda_i^{\rho_i}(\mathbf{p}) = \frac{\rho_i(\boldsymbol{\gamma}^{(i)} \cdot \mathbf{p} + m_i) + \omega_i \gamma_0^{(i)}}{2\omega_i}. \quad (2.4)$$

Let us define the eigenstates of these projection operators by

$$\Lambda^{\rho_1\rho_2} \gamma_0^{(1)} \gamma_0^{(2)} |\rho_1\rho_2\rangle_{pw} = |\rho_1\rho_2\rangle_{pw}. \quad (2.5)$$

The subscript pw is used to distinguish these plane wave states from the canonical positive and negative states defined through

$$\gamma_0^{(1)} \gamma_0^{(2)} |\rho_1\rho_2\rangle_{ca} = \rho_1 \rho_2 |\rho_1\rho_2\rangle_{ca}, \quad (2.6)$$

which correspond to the various combinations of upper and lower components of the Dirac spinors. Clearly

$$|\rho_1\rho_2\rangle_{pw} = |\rho_1\rho_2\rangle_{ca} + \mathcal{O}(p/m). \quad (2.7)$$

The instantaneous interaction V between the quarks is modeled as the sum of a Coulomb-like part describing the one-gluon-exchange (OGE) interaction and a linearly rising part for the confinement. It takes in coordinate space the form

$$V(x) = -\frac{\alpha(x)}{x} \Gamma_V + (\kappa x + c) \left[(1 - \varepsilon) \mathbf{1}^{(1)} \mathbf{1}^{(2)} + \varepsilon \Gamma_V \right]. \quad (2.8)$$

The vector contribution to the interaction is studied in the Feynman gauge as well as in the Coulomb gauge:

$$\Gamma_V^{Feynman} = \gamma_\mu^{(1)} \gamma^\mu (2), \quad (2.9)$$

$$\Gamma_V^{Coulomb} = \gamma_\mu^{(1)} \gamma^\mu (2) + \frac{1}{2} \left[\boldsymbol{\gamma}^{(1)} \cdot \boldsymbol{\gamma}^{(2)} - (\boldsymbol{\gamma}^{(1)} \cdot \hat{\mathbf{x}})(\boldsymbol{\gamma}^{(2)} \cdot \hat{\mathbf{x}}) \right]. \quad (2.10)$$

This defines the relativistic quasi-potential model. Note that we do allow for a fraction ε of vector-confinement. The running coupling constant behaves as $\alpha(x) \sim (8/27)\pi/\ln(x_0/x)$ for small distances x , and grows to some maximum saturation value α_{sat} for large separations, according to the interpolation given in I.

The resulting wave equation were studied extensively in coordinate space. It should be noted that certain difficulties as found in the one particle Dirac equation should be expected in such a relativistic quasi-potential approach. Let us for a moment consider one fermion in an external potential. If this particle experiences a potential which fluctuates

more strongly than $\sim 2m$ over a distance shorter than its Compton length $x_C = 1/m$ new fermion-antifermion pairs can be created. This phenomenon cannot correctly be described by the Dirac equation which describes a one-particle theory and thus misses the interactions between the newly created pair and the starting particle. Since the Dirac equation does allow for antifermion components, solutions in this potential can have an unbound number of non-interacting fermions and antifermions thus being unnormalizable and unphysical. This break-down of the Dirac equation is well-known as the Klein paradox [7]. Similar flaws emerge in the QP equations of this work since they also contain negative energy components. In view of the complexity of the various two-body equations we do not fully analyze under what conditions they break down. Instead, let us note that unbound solutions can be expected if the confining strength becomes too strong, $\kappa x_C \gtrsim 2m$ or $\kappa \gtrsim 2m^2$. This domain can be reached in light meson systems. The condition on κ depends on the fraction ε of vector confinement as indicated by the discussion in I. Similarly, if the OGE potential becomes too strong, $\alpha/x_C \gtrsim 2m$ or $\alpha \gtrsim 2$, irregular solutions may be expected. Mesons with high orbital angular momenta are less sensitive to this effect because the centrifugal barrier prevents them from entering the short distance region. If a running coupling constant is taken instead of a fixed one then the irregular solutions disappear and the singular behavior becomes less. Whereas the upper bound on κ disappears as the negative energy components are removed, the upper bound on α is shifted upward but still present, reflecting that only positive energy states can also tumble in a OGE potential. Detailed discussions on the short distance behavior was given in I and II.

III. RESULTS

Since the wave equations as described in the previous section are solved in the coordinate space using the representation of the canonical states Eq. (2.6), a convenient way to switch off the coupling to the negative energy plane wave states is to explicitly project out these states in the interaction. The projection is done by rewriting the BSLT equation as

$$\begin{aligned} & [(\omega - E)\Lambda^{++} - E(\Lambda^{+-} + \Lambda^{-+}) - (i_{bb}\omega + E)\Lambda^{--}] \psi = \\ & -\frac{1}{4\omega} [(\omega + E)\Lambda^{++} + i_b E(\Lambda^{+-} + \Lambda^{-+}) + i_{bb}(E - \omega)\Lambda^{--}] \gamma_0^{(1)} \gamma_0^{(2)} V \psi. \end{aligned} \quad (3.1)$$

For $i_b = i_{bb} = 1$ we recover the QP equations with all negative energy states included. If i_b is put to zero then the single negative energy states are projected to zero, provided $E \neq 0$, and similarly for i_{bb} when we want to drop the coupling to the $|--\rangle_{pw}$ states in the calculations. One can rewrite the ET equation in a similar way:

$$\begin{aligned} & 2 [(\omega - E)\Lambda^{++} - \omega(\Lambda^{+-} + \Lambda^{-+}) + (i_{bb}\omega + E)\Lambda^{--}] \psi = \\ & - [\Lambda^{++} + i_b(\Lambda^{+-} + \Lambda^{-+}) + i_{bb}\Lambda^{--}] \gamma_0^{(1)} \gamma_0^{(2)} V \psi. \end{aligned} \quad (3.2)$$

Although the number of coupled channels do not change, the above Eqs. (3.1) and (3.2) have a major advantage that they can be solved in the same way as the full BSLT and ET equations were solved in I. First we Fourier transform them to configuration space and make an angular momentum decomposition. This gives a set of coupled integral-differential

equations which are reduced to a set of linear equations by expanding the wave function on a set of spline functions. The resulting matrix equation for the various spline coefficients can be solved straightforwardly by standard methods. As a check on the accuracy of our calculational procedures we used this method to calculate the charmonium mass spectrum in the model of Hirano *et al.* [8], which includes only the $|++\rangle_{pw}$ and $|--\rangle_{pw}$ states. Agreement was found within 1 MeV.

A. Comparison with Schrödinger equation results

To study the effects of various relativistic contributions we consider the mass spectra for the light mesons and the charmonium system. In the limit of large quark masses the BSLT can be reduced to the nonrelativistic Schrödinger equation

$$\left[2 \left(-\frac{\nabla^2}{2m} + m \right) + V_{NR}(x) + V_{SD}(x) \right] \psi(x) = M\psi(x), \quad (3.3)$$

where V_{NR} is the nonrelativistic reduction of the potential

$$V_{NR}(x) = -\frac{\alpha(x)}{x} + \kappa x + c, \quad (3.4)$$

and V_{SD} contains the spin-dependent corrections of order $1/m^2$ [9]

$$\begin{aligned} V_{SD}(x) &= \frac{1}{m^2} \left[\frac{3V'_V - V'_S}{2x} \mathbf{L} \cdot \mathbf{S} + \frac{2}{3} (\nabla^2 V_V) \mathbf{S}_1 \cdot \mathbf{S}_2 + \left(\frac{1}{x} V'_V - V''_V \right) S_{12} \right], \\ S_{12} &= (\mathbf{S}_1 \cdot \hat{\mathbf{x}})(\mathbf{S}_2 \cdot \hat{\mathbf{x}}) - \frac{1}{3} \mathbf{S}_1 \cdot \mathbf{S}_2. \end{aligned} \quad (3.5)$$

Here V_V and V_S denote the vector and scalar contributions to the potential. The potential in Eq. (3.5) is singular at the origin and therefore a regularization is needed. The delta function appearing in $\nabla^2 V_V$ is replaced by a gaussian of width β_1^{-1} , and the x^{-1} - and x^{-3} -singularities are cut off at $x_0 = \beta_2^{-1}$ and replaced by smoothly fitting gaussians. We take the same parameters for the potential as in I, which are summarized in table 1, and take the β_i such that they reproduce approximately the same splittings between the S - and P -states as the full BSLT calculation. With these parameters we find the spectra as shown in the first column of Figs. 1 and 2 of the $u\bar{u}$ and $c\bar{c}$ systems. The spectra of the various columns in these figures will be referred to as Fig. 1a, 1b, ... etc.

The first natural step in relativizing the Schrödinger equation is to replace the kinetic energy according to

$$\frac{\mathbf{p}^2}{2m} + m \rightarrow \omega = \sqrt{\mathbf{p}^2 + m^2} \quad (3.6)$$

in Eq. (3.3). Figs. 1b and 2b show the corresponding spectra. They are shifted downwards as compared to the nonrelativistic ones indicating that the interaction has become more attractive. Also the shift becomes larger as the level of excitation increases. For charmonium

one finds shifts between $0.05 - 0.13$ GeV, whereas for the light mesons these shifts are more substantial and range between $0.5 - 1.5$ GeV.

The second relativistic correction which can be included is to replace the approximation of the potential $V_{NR} + V_{SD}$ by the complete projection of the potential Eq. (2.8) on positive energy states $V^{++,++} \equiv {}_{pw}\langle ++|V\gamma_0^{(1)}\gamma_0^{(2)}|++\rangle_{pw}$. The singular behavior of V_{SD} is no longer present in the complete projection, and hence the cut-off parameters β_i are principally absent in the resulting wave equations. Note the factors $\gamma_0^{(1)}\gamma_0^{(2)}$ in $V^{++,++}$ and in the right hand sides of Eqs. (3.1) and (3.2) which reflect that the energies of the quarks are the fourth components of their four-momenta. This replacement gives a rather large effect ($0.00 - 0.16$ GeV for $c\bar{c}$ and $0.0 - 0.8$ GeV for $u\bar{u}$) as is illustrated by the spectra in Fig. 1c and 2c and which is easily understood. For a potential $V(x) = V_S(x)\mathbf{I} + V_V(x)\gamma_0^{(1)}\gamma_0^{(2)}$ and low momenta of the in- and outgoing states

$$V^{++,++} \approx {}_{ca}\langle ++|V_S\gamma_0^{(1)}\gamma_0^{(2)} + V_V(x)\mathbf{I}|++\rangle_{ca} = V_S(x) + V_V(x). \quad (3.7)$$

But for relativistic momenta considerable contributions to $V^{++,++}$ are to be expected from the contributions

$${}_{ca}\langle -+|V_S\gamma_0^{(1)}\gamma_0^{(2)} + V_V(x)\mathbf{I}|-\rangle_{ca} = -V_S(x) + V_V(x). \quad (3.8)$$

For scalar confinement it leads to a considerable reduction of the confinement strength. This effect can also qualitatively be seen from the spin-independent corrections of order $1/m^2$ [9] to a nonrelativistic scalar potential. It is given by

$$V_{SI}(x) = \frac{1}{m^2} \left[\frac{1}{4}(\nabla^2 V_S) + V'_S \frac{d}{dx} + V_S \nabla^2 \right]. \quad (3.9)$$

This potential, however, does not give an accurate approximation since for large distances $m^{-2}V_S \nabla^2$ is not a small enough parameter to expand in.

To obtain the explicit form of the BSLT propagator we may replace

$$(\omega - E) \rightarrow \frac{2\omega}{\omega + E}(\omega - E). \quad (3.10)$$

This leads to the BSLT equation restricted to only positive energy states. Figs. 1d and 2d show how the masses are increased.

Figure 1e shows the effect of the introduction of the single negative energy states $|+-\rangle_{pw}$ and $|-\rangle_{pw}$. For the light mesons we do not show this case since for some mesons it leads to unbound systems, similar to the Klein paradox mentioned in the previous section. The introduction of these states leads to an increase of the $c\bar{c}$ spectrum by up to 0.10 GeV. They are mostly made out of $|+-\rangle_{ca}$ and $|-\rangle_{ca}$ states which have a negative expectation value of scalar confinements, Eq. (3.8). Together with the negative propagation of these states this leads to a positive interaction which raises the mass levels.

Finally, if the $|-\rangle_{pw}$ states are included, one arrives at the full BSLT spectra shown in Figs. 1f and 2e. The inclusion of these states changes little ($\lesssim 1$ MeV for $c\bar{c}$), as could be expected from their smallness. The lowest lying mesons, however, are considerably influenced what is related to the singular behavior of the wave function at small distances.

The OGE potential concentrates the wave function to small distances with strong potential, thus lowering the mass levels. The singular behavior becomes stronger if more negative energy states are included or if the level of excitation is less. Fig. 1g shows the charmonium spectrum in the Salpeter approximation, which includes only the $|++\rangle_{pw}$ and $|--\rangle_{pw}$ states. The small masses for the low lying excitations are still present, but the increase associated with the single negative states is absent.

B. Equal-time results

Let us briefly discuss what effects are found if we use the equal time (ET) propagator. In Fig. 3 is shown the corresponding charmonium spectrum calculated with the same parameters as Fig. 1. Three differences can be noted. Firstly, the ET spectrum is lowered as compared to the BSLT one. This is a consequence of the different propagators for the $|++\rangle_{pw}$ states [cf. Eq. (3.10)]. Secondly, the introduction of the single negative energy states causes a shift upwards in the ET model which is approximately twice that seen in BSLT. This is due to the fact that these states are roughly twice as important in the ET wave function as in the BSLT one in view of a twice as large propagator for these states, $S_{ET}^{++} = -1/2\omega$ versus $S_{BSLT}^{++} = -1/4\omega$. Thirdly, the $|--\rangle_{pw}$ energy states lower the singlet states much more strongly in the ET model than in BSLT. Again, this is a consequence of the importance of these states in the ET wave function. They are larger due to the large S_{ET}^{--} propagator. As already remarked in [6], this is a defect of the ET equation when an unretarded potential is used, and this disappears if the proper retardation is inserted in the matrix elements for V that connect to double negative energy states. However, it should be stressed that there is no unambiguous extension of the instantaneous confining potential to retarded times.

C. Sensitivity to vector confinement

In I we discussed the large raising of the light meson spectrum when a part of vector confinement is added to a scalar confining potential. Fig. 4 shows the $u\bar{u}$ spectrum for various dynamical models using scalar confinement without and with a vector contribution. When only positive energy states are taken the raising is even more stronger, and can almost double some meson masses.

In Fig. 4 are also shown the same spectrum if the vector contribution is taken in the Feynman gauge, Eq. (2.9). In this gauge the spin-spin interaction is less suppressed so the vector contribution has more effect.

IV. CONCLUDING REMARKS

In summary, we have calculated for the light and charmonium systems mass spectra using the (relativized) Schrödinger equation and the relativistic quasi-potential equations of I and II, which differ from the Schrödinger approach in that no $1/m^2$ approximation is made, and that the QP equations contain the full Dirac structure of positive and negative energy states. We studied the importance of these differences by solving the QP equations

while leaving out negative energy components. We find that the projection of the confining potential on positive energy states leads to a considerably lower confinement strength than the nonrelativistic potential gives. This is partly compensated for by the introduction of the single negative energy states which are more bound than the positive states, and hence increase the masses. Finally we find that the double negative energy states have little influence except for short distances where the singular behavior of the mesons is strengthened.

The total picture strongly suggests that the differences here studied are important for determining the parameters of the $q\bar{q}$ interaction, especially the confinement strength κ . Yet the global structure of the spectrum —level ordering, relative sizes of splittings— remains rather untouched under the relativistic modifications. This confirms the conclusion drawn from the success of nonrelativistic quark models that most relativistic effects in $q\bar{q}$ spectroscopy can be mimicked by employing nonrelativistic dynamics together with effective parameters. It will be interesting to study whether the relativistic modifications to meson wave functions will lead to sizeable changes in cross section for processes such as e.m. ones involving these mesons.

In this paper we have studied relativistic effects within the framework of quasi-potential equations. In so doing we have not addressed entirely the role of the relative energy variable p_0 . Apart from the complexity of a calculation including this say in a Bethe-Salpeter equation approach, a more fundamental obstacle is posed by the extension of the definition of the confining potential, as we have used here, to a four-momentum dependence. The confining potential is only known for the static case. There is at this moment no underlying theory which can give a prescription on how to extend it to a covariant form. Let us illustrate this considering the commonly used generalization of the potential $V(x) = \kappa x$ which reads in momentum space

$$V(q_0, \mathbf{q}) = \frac{\kappa}{2\pi^2} \lim_{\eta \rightarrow 0} \left[\frac{\partial^2}{\partial \eta^2} \frac{1}{\mathbf{q}^2 - q_0^2 + \eta^2(1 - i\varepsilon)} \right], \quad (4.1)$$

but its Fourier transform yields

$$V(t, x) = \frac{\kappa}{\pi} \lim_{\eta \rightarrow 0} [K_0(\eta R) - \eta R K_1(\eta R)] = \infty, \quad (4.2)$$

(with $R^2 = x^2 - t^2$) which is clearly physically unacceptable. Exploring QCD may lead to ways of reconstructing such a confining force, which can be used in such an off mass shell approach as we have discussed here.

ACKNOWLEDGMENTS

This work was partially financially supported by de Stichting voor Fundamenteel Onderzoek der Materie (FOM), which is sponsored by the Nederlandse Organisatie voor Wetenschappelijk Onderzoek (NWO).

REFERENCES

- [1] P.C. Tiemeijer and J.A. Tjon, Utrecht preprint THU-92/31, nucl-th 9211003.
- [2] P.C. Tiemeijer and J.A. Tjon, Phys. Lett. B 277 (1992) 38.
- [3] R. Blankenbecler and R. Sugar, Phys. Rev. 142 (1966) 1051; A.A. Logunov and A.N. Tavkhelidze, Nuovo Cimento 29 (1963) 380.
- [4] E.D. Cooper and B.K. Jennings, Nucl. Phys. A 500 (1989) 553.
- [5] V.B. Mandelzweig and S.J. Wallace, Phys. Lett. B 197 (1987) 469; S.J. Wallace and V.B. Mandelzweig, Nucl Phys A 503 (1989) 673.
- [6] S.J. Wallace in Nuclear and Particle Physics on the Light Cone, Proceedings of the LAMPF Workshop, Los Alamos 1988.
- [7] see e.g. J.D. Bjorken and S.D. Drell, Relativistic quantum mechanics (McGraw-Hill, New York, 1964).
- [8] M. Hirano, K. Iwata, K. Kato, T. Murota and D. Tsuruda, Prog. Theor. Phys. 69 (1983) 1498.
- [9] W. Lucha, F.F. Schöberl and D. Gromes, Phys. Rep. 200 (1991) 127.

FIGURES

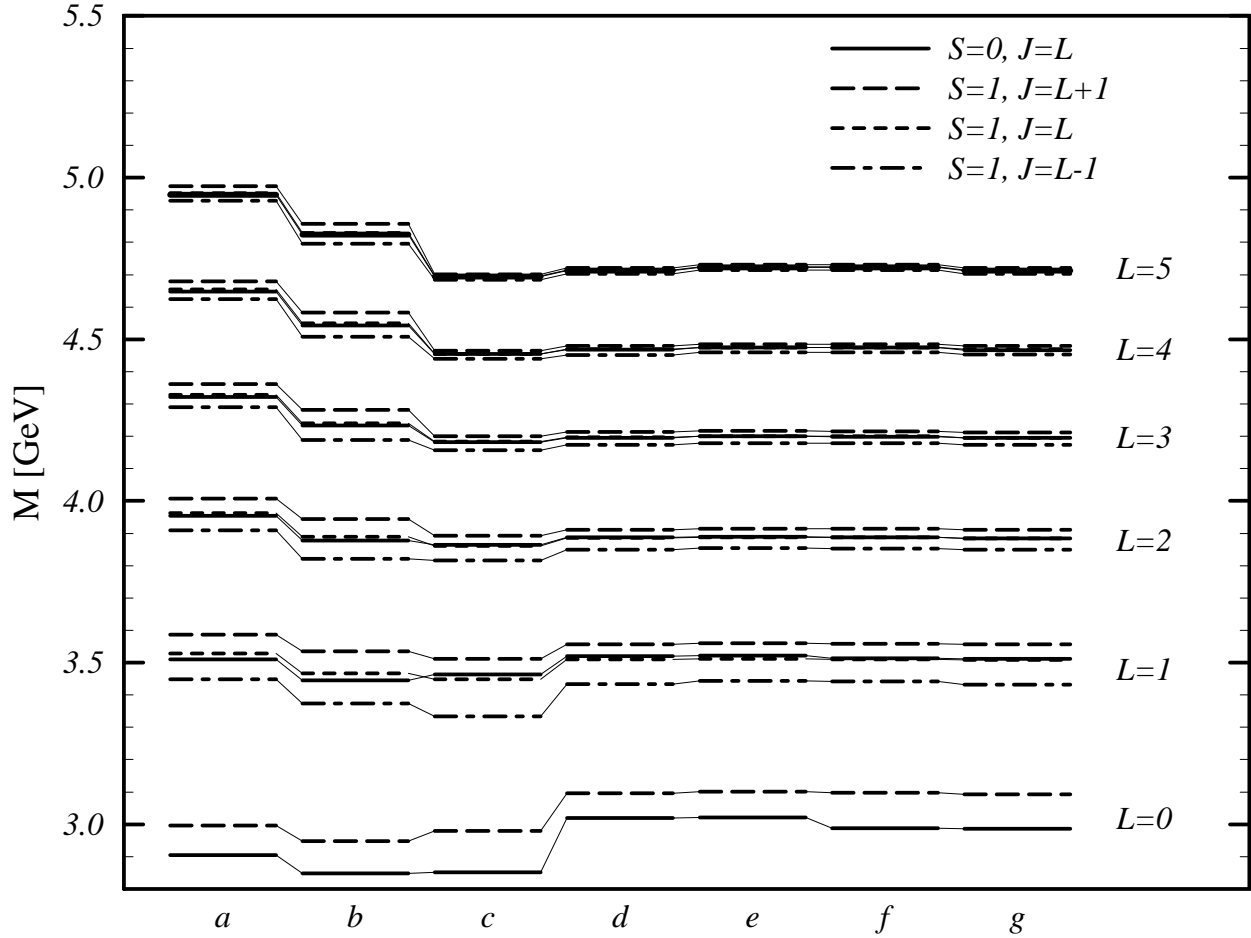


FIG. 1. Charmonium spectrum of the radially unexcited states. a: Schrödinger equation with $p^2/2m$ and Breit interaction, b: Schrödinger equation with $\sqrt{p^2 + m^2}$ and Breit interaction, c: Schrödinger equation with $\sqrt{p^2 + m^2}$ and full projection of potential in Coulomb-gauge, i.e. ET with $|++\rangle_{pw}$, d: BSLT with $|++\rangle_{pw}$, e: BSLT with $|++\rangle_{pw}$, $|+-\rangle_{pw}$ and $|--\rangle_{pw}$, f: BSLT with all states, g: BSLT with $|++\rangle_{pw}$ and $|--\rangle_{pw}$.

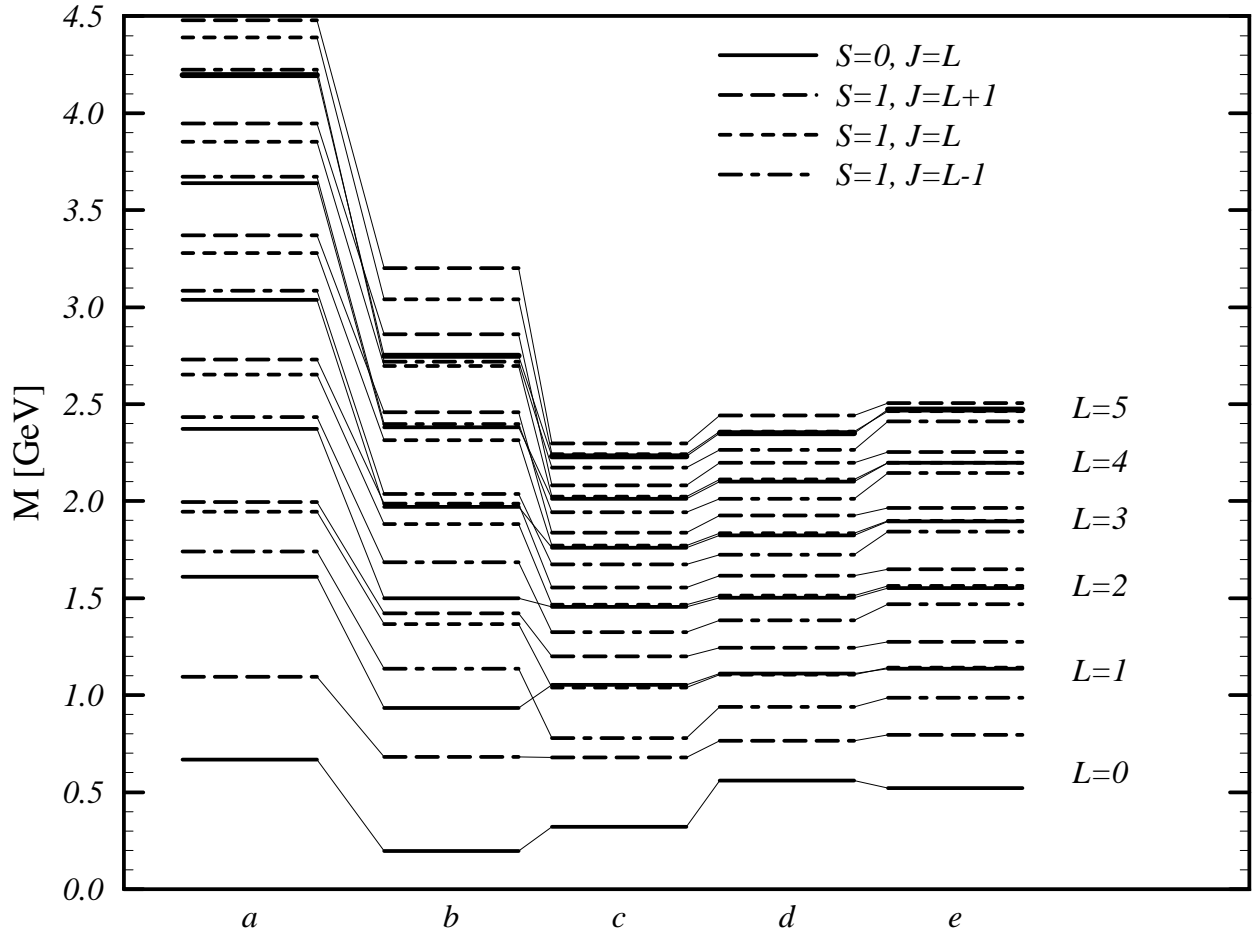


FIG. 2. Light meson spectrum of the radially unexcited states. a: Schrödinger equation with $p^2/2m$ and Breit interaction, b: Schrödinger equation with $\sqrt{p^2 + m^2}$ and Breit interaction, c: Schrödinger equation with $\sqrt{p^2 + m^2}$ and full projection of potential in Coulomb-gauge, i.e. ET with $|++\rangle_{pw}$, d: BSLT with $|++\rangle_{pw}$, e: BSLT with all states.

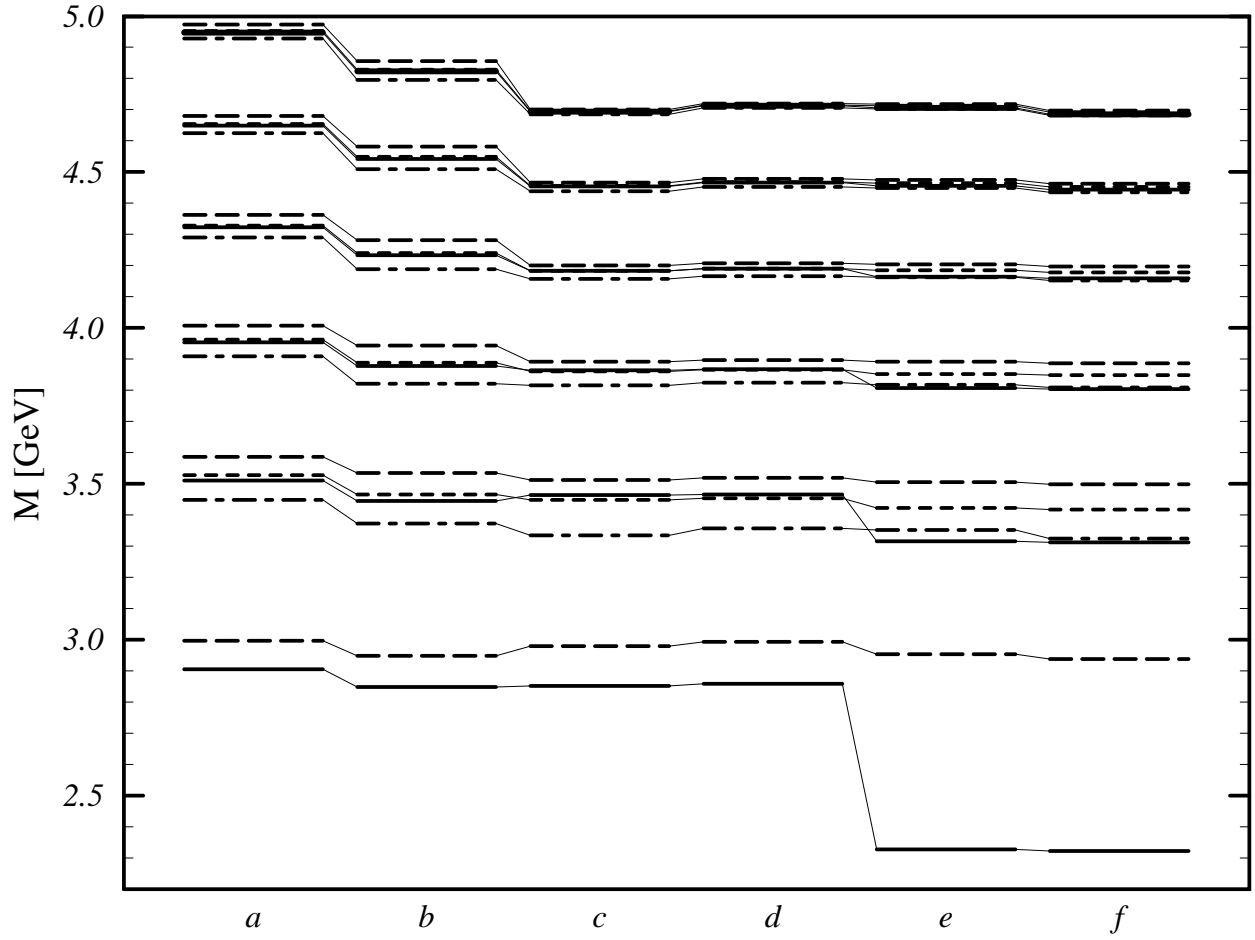


FIG. 3. Charmonium spectrum of the radially unexcited states (legend as in Fig. 1).
 a: Schrödinger equation with $p^2/2m$ and Breit interaction, b: Schrödinger equation with $\sqrt{p^2 + m^2}$ and Breit interaction, c: Schrödinger equation with $\sqrt{p^2 + m^2}$ and full projection of potential, i.e. ET with $|++\rangle_{pw}$, d: ET with $|++\rangle_{pw}$, $|+-\rangle_{pw}$ and $|--\rangle_{pw}$, e: ET with all states, f: ET with $|++\rangle_{pw}$ and $|--\rangle_{pw}$.

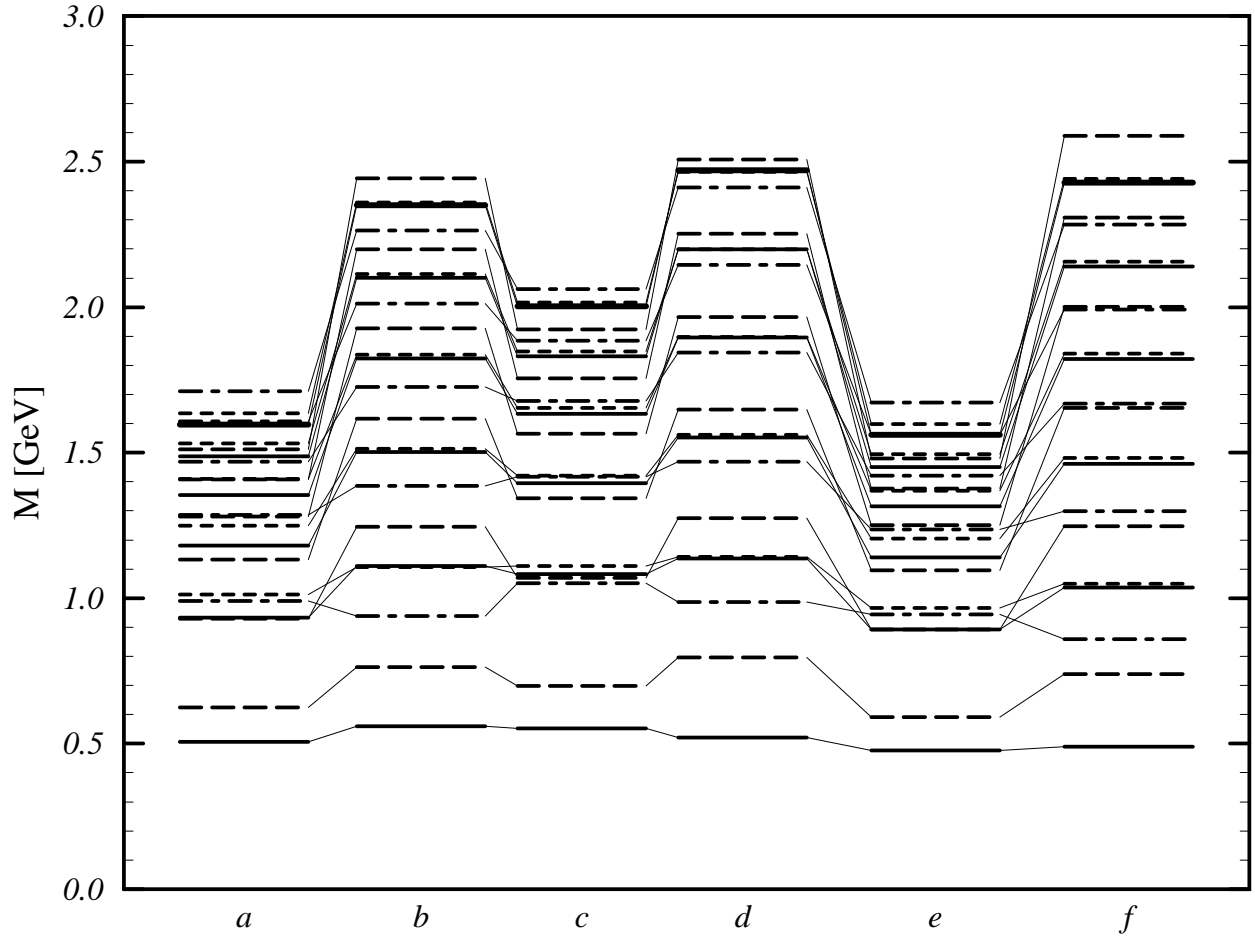


FIG. 4. Light meson spectrum of the radially unexcited states (legend as in Fig. 1). a: BSLT in Coulomb gauge with $|++\rangle_{pw}$ and $\varepsilon = 0$, b: BSLT in Coulomb gauge with $|++\rangle_{pw}$ and $\varepsilon = 0.25$, c: BSLT in Coulomb gauge with all states and $\varepsilon = 0$, d: BSLT in Coulomb gauge with all states and $\varepsilon = 0.25$, e: BSLT in Feynman gauge with $|++\rangle_{pw}$ and $\varepsilon = 0$, f: BSLT in Feynman gauge with $|++\rangle_{pw}$ and $\varepsilon = 0.25$.

TABLES

TABLE I. Parameters for the $q\bar{q}$ model

	u \bar{u}	c \bar{c}	
m	0.250	1.779	GeV
κ	0.33	0.33	GeV 2
c	-1.0	-1.0	GeV
ε	0.25	0.25	
α_{sat}^a	0.8	0.8	
β_1	0.25	0.8	GeV
β_2	0.10	0.6	GeV

^aRunning as α_I in Ref. [1] with $\mu = 1.0$